D_{5h} C_{50} Fullerene: A Building Block for Oligomers and Solids?

Lyuben Zhechkov, Thomas Heine,* and Gotthard Seifert

Institut für Physikalische Chemie und Elektrochemie, TU Dresden, D-01062 Dresden, Germany

Received: August 16, 2004; In Final Form: October 14, 2004

The particular stability of recently synthesized $C_{50}Cl_{10}$ cage is discussed by means of its topology: the underlying C_{50} cage consists of two corannulene frameworks which are connected by five C_2 units. $C_{50}X_{10}$ is another lower fullerene which has not been found experimentally in its bare form. Oligomerization and polymerization of C_{50} and $C_{50}H_x$ are investigated. A minimum energy pathway to a D_{5h} $(C_{50})_6H_{40}$ structure is found. C_{50} is a candidate structure to form oligomers and fullerides. The preferred bridging positions and the 5-fold symmetry suggest the formation of irregular polymers and oligomers.

Introduction

Fullerenes, as fourth allotrope of carbon, have caught the attention of chemists, physicists and material scientists since the 1980s. Immense progress was achieved in fullerene characterization and preparation. A manifold of the so-called IPR (isolated-pentagon rule[1,2]) fullerenes, starting with C_{60}, C_{70}, and C_{70+2n}, $n = 1, 2, ...$, has been produced and studied both experimentally and theoretically.[3−6] Since 1998, smaller fullerenes, which violate the IPR, have been reported,[7,8] and even the smallest possible fullerene, C_{20}, containing only pentagons and no hexagons, has been synthesized, but with a lifetime on the μs time scale.[9] In contrast to IPR fullerenes, the small fullerenes have been found to be highly reactive, and for example C_{36} was only isolated in its chemically saturated form as a fullerene hydride or oxyhydride.[8,10,11]

The high reactivity of smaller fullerenes makes them excellent candidates to form covalently bound fullerene solids. As the frontier orbitals of fullerenes are determined by their π systems, which are themselves strongly influenced by the bonding patterns of the fullerenes, the connectivity of a fullerene solid determines its structural, mechanical, and electronical properties on a large extent. Fullerene solids (fullerides) are good candidates to form super-hard, lightweight materials with high-temperature resistance and with interesting electronic properties. Carbon can be tri- or tetravalent in these solids, which allows a large manifold of possible structures.[8,12−16]

Recently, a cage based on a D_{5h} C_{50} fullerene, D_{5h} $C_{50}Cl_{10}$, has been reported.[17] Similar to C_{36}, it is readily forming a chemically saturated configuration. The structure has been unambiguously characterized by measured and simulated ^{13}C NMR,[17] and electronic properties of this fullerene have been studied recently.[18,19]

In this article, we want to discuss several issues on D_{5h} C_{50}: Is this particular isomer special within the 271 classical C_{50} fullerenes? We provide a simple explanation of the high stability of this cage. So far, reactive lower fullerenes have always been candidates for the formation of fullerides.[8,20] The formation of fullerides on the basis of the reported D_{5h} cage is therefore to be expected, and we evaluate possible connectivity patterns to form dimers and oligomers. Finally, the possibility to form fullerene solids based on C_{50} is discussed.

* To whom correspondence should be addressed. Fax: +49 351 463 35935. E-mail: thomas.heine@chemie.tu-dresden.de.

TABLE 1: Relative Energies of C_{50} Isomers[a]

S	point group	e_{55}	E_{DFTB}	$E_{PBE/DZVP//DFTB}$	$E_{B3LYP/6-31G*//DFTB}$	$E_{B3LYP/6-31G*}$[19]
271	D_{5h}	5	0.0	0.0	0.0	0.0
270	D_3	6	14.1	−32.7	−9.0	−9.6
266	C_s	6	44.5	3.8	37.0	24.3
264	C_s	6	86.8	39.6	72.7	66.2
263	C_2	6	57.7	13.0	38.6	
262	C_s	6	100.8	80.4	96.2	93.8
260	C_2	6	94.0	62.7	88.2	85.4

[a] Labeled using the spiral numbering *S*,[22] see Figure 1. Relative energies are given in kJ/mol. The B3LYP/6-31G* values are taken from ref 19.

Computational Details

Topological structures of all classical C_{50} isomers have been taken from the "Fullerene Structure Library".[21] They have been generated using the spiral algorithm and are labeled in the spiral nomenclature.[22] All geometries were fully optimized using the DFTB method.[23] Relative energies of selected isomers have been computed at optimized DFTB geometries using the gradient-corrected local density approximation proposed by Perdew, Burke, and Ernzerhof (PBE)[24] with a double-ζ basis set including polarization functions[25] using the deMon 2004 code.[26] Additionally, energies of selected structures have been computed using the B3LYP hybrid functional in combination with a 6-31G* basis as implemented in Gaussian[27] to allow comparison with reported values by Lu et al.[19] C_{50} dimers and oligomers have been pre-optimized with a force field.

Monomers: C_{50}, $C_{50}H_{10}$, $C_{50}Cl_{10}$, $C_{50}H_x$. Graph theory reports 271 possible isomers of classical C_{50} fullerenes, i.e., such which contain only 12 pentagonal and 10 hexagonal rings.[22] The complete set of 271 geometries have been fully optimized using the DFTB method. Seven isomers have relative energies of about 100 kJ/mol (see Table 1) with respect to the most stable cage (shown in Figure 1). The isomer with the lowest number of pentago*n*-pentagon adjacencies (e_{55}) is D_{5h} C_{50}:271 (in spiral nomenclature) and is found to be the most stable classical C_{50} fullerene within the DFTB method. The second isomer, D_3 C_{50}: 270, has six e_{55} and is found to be 14 kJ/mol less stable. Single-point GGA-DFT calculations on optimized DFTB geometries (PBE/DZVP//DFTB and B3LYP/6-31G*//DFTB, this notation, which gives the computational level of the energy computation // computational level of the geometry optimization, will be used throughout in the following) find the isomer order of the two most stable isomers reversed, and the D_3 cage is slightly (9 kJ/

10.1021/jp046318l CCC: $27.50
Published on Web 12/04/2004

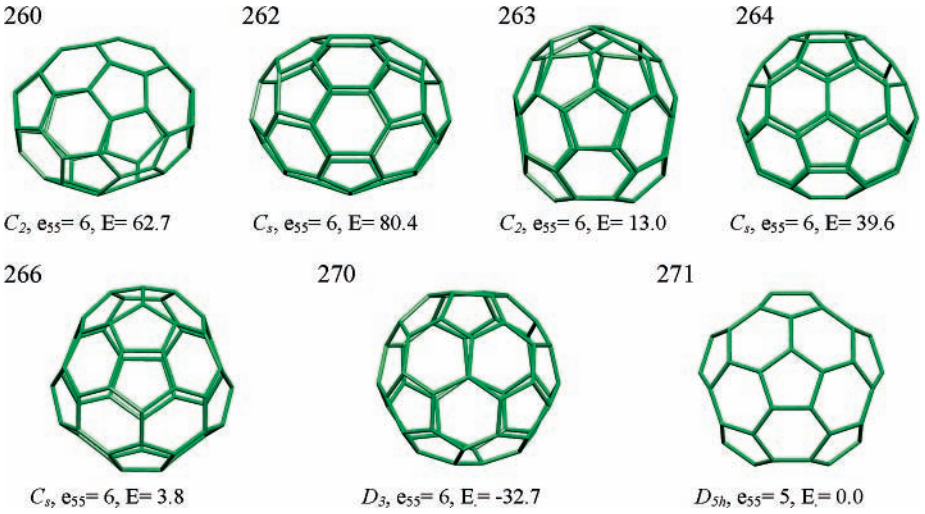

Figure 1. Structures (label in spiral notation[22]), geometry, point group, number of pentago*n*-pentagon adjacencies e_{55} and relative energies at the PBE/DZVP//DFTB level (in kJ/mol) of classical C_{50} isomers of lowest relative energy.

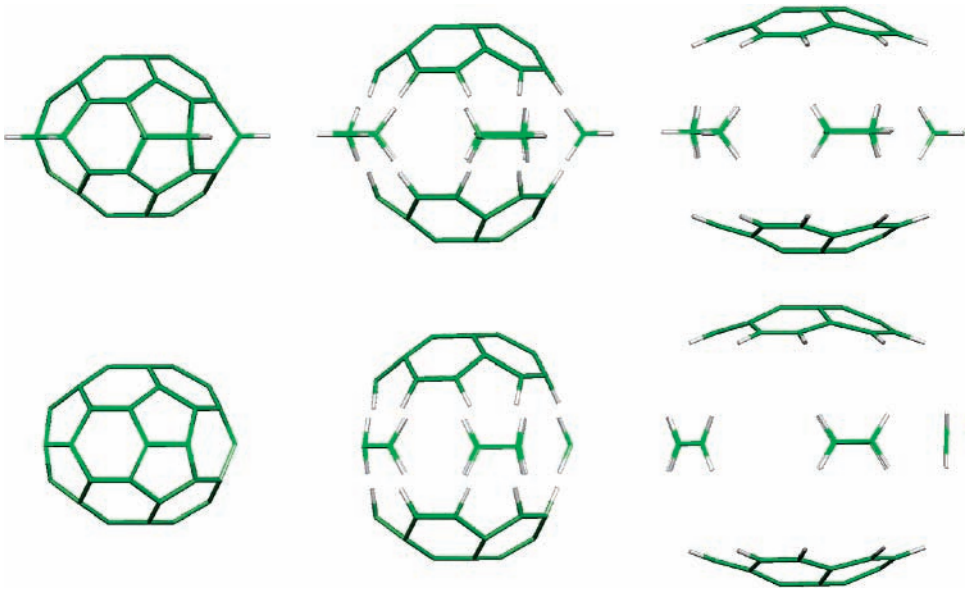

Figure 2. $C_{50}H_{10}$ (top) and C_{50} (bottom), decomposed into frozen (center) and optimized (right) corannulene and C_2H_6/C_2H_4 units, respectively. The energy difference of the frozen parts (center) and the optimized parts (right) is the strain energy of the cages. The difference between the strain energies of the two cages corresponds to the release of strain energy by hydrogenation of the bare cage to $C_{50}H_{10}$.

mol) more stable than D_{5h} isomer 271 (Table 1). Relative energies of some classical C_{50} isomers have been studied before by other groups and are in agreement with our DFT values[19,28] (see Table 1). However, the two most stable isomers are nearly isoenergetic. The inherent errors of the applied and even higher-level quantum chemistry methods are much larger than those small relative energy differences,[13,29] and hence characterization has to be supported by additional information, e.g., ^{13}C NMR spectroscopy.

In contrast to previous studies,[7,13,30] the "rule of minimal pentagon−pentagon adjacencies"[30] is violated for C_{50}:D_{5h} C_{50}: 271 has the lowest number of five pentagon−pentagon adjacencies and is found to be 9.6 kJ/mol (2.3 kcal/mol) less stable then the competing D_3 isomer (6 pentago*n*-pentagon adjacencies).[19] As the introduction of an additional pentago*n*-pentagon adjacency in lower fullerenes is usually giving a large energy penalty of ∼80−100 kJ/mol,[30] the D_{5h} structure must have an exceptionally high strain energy to have a comparable energy as C_{50}:270. Indeed, D_{5h} C_{50} (Figure 2) has the structure of two corannulene frameworks, glued together with 5 C_2 units in the sigma plane, which we refer below as "equatorial belt". The C−C bonds of the 5 C_2 units are the bonds between two adjacent pentagons.

In experiment, only saturated $C_{50}Cl_{10}$, but not C_{50}, has been found.[17] D_{5h} C_{50} and $C_{50}Cl_{10}$, respectively, have four distinct carbon atoms in their cages, confirmed by the experimental four-line ^{13}C NMR spectrum shows, which are in agreement with quantum-chemical computations of D_{5h} $C_{50}Cl_{10}$ within an accuracy of 2 ppm.[17] Hence, the isomer is unambiguously assigned. The 10 Cl atoms are bound to the 5 C_2 units at the equatorial belt and stabilize the cage in two ways: First, they decrease the strain energy of the cage by pyramidalization of the equatorial carbons to sp^3, and second they take the carbons of adjacent pentagons out of the π system and hence give electronic stabilization.

In this vein, C_{50} is somewhat similar to C_{36}, which was also never detected as a bare fullerene, not even in the mass spectrum,[8,17] but fullerene hydrides[8] and oxyhydrides[10,11] have been reported on the basis of C_{36}. The cage found in experiment is not the most stable bare fullerene cage predicted by theory.[13,31−33]

TABLE 2: Geometries of Related $C_{50}H_{10}$, $C_{50}Cl_{10}$, and C_{50} (Based On D_{5h} C_{50}:271) Cages at the Fully Optimized B3LYP/6-31G* Level (in Å)[a]

bonds	$C_{50}H_{10}$	$C_{50}Cl_{10}$	C_{50}
1−1	1.439	1.463	1.465
1−2	1.406	1.423	1.390
2−3	1.435	1.457	1.469
3−3	1.378	1.393	1.415
3−4	1.533	1.557	1.417
4−4	1.577	1.626	1.470

[a] Bond types are given in Figure 3.

Figure 3. Labeling of D_{5h} C_{50}:271.

The addition patterns are characteristic for each cage topology, as it reduces strain and stabilizes the π system.[12−14,17,34]

In agreement with recent computations of Lu et al.,[19] we find that saturation of D_{5h} C_{50} with Cl and with H gives comparable molecular stability of the saturated cages, and the cage frameworks of $C_{50}Cl_{10}$ and $C_{50}H_{10}$ show very similar geometries (see Table 2).

The strain of C_{50} and $C_{50}H_{10}$ has been compared in the following procedure: The corannulene framework was taken out of the cage, frozen, and the cut C−C bonds were saturated with hydrogen. The C_2/C_2H_2 units (in case of $C_{50}/C_{50}H_{10}$, respectively) of the equatorial belt were treated in the same way. The bond lengths of the saturated hydrogen atoms were determined by restricted geometry optimization and the strain was calculated by comparison of the energy with respect to two free corannulene and five free C_2H_4/C_2H_6 for $C_{50}/C_{50}H_{10}$, respectively (Figure 2). We estimate the strain energy to be 2213 kJ/mol for the bare fullerene, and find a strongly reduced value for $C_{50}H_{10}$ at 941 kJ/mol at the B3LYP/6-31G* level.

The electronic stabilization is illustrated by the HOMO−LUMO gaps and the electronic states of C_{50}, $C_{50}Cl_{10}$, and $C_{50}H_{10}$. The electronic structures of $C_{50}Cl_{10}$ and $C_{50}H_{10}$ are very similar, whereas C_{50} and the saturated molecules differ strongly. The gap energy increases from 1.4 eV for C_{50} to 3.5 eV for $C_{50}H_{10}$/3.1 eV for $C_{50}Cl_{10}$. For C_{50}, the HOMO is a single orbital which is localized at the equatorial carbon atoms. This orbital becomes a σ orbital when the molecule is saturated and does not appear any more among the higher occupied orbitals. These orbitals also have π character for the saturated species, but they are always degenerate.

As the next step, we investigate the influence of removing two H atoms from different sites of the equatorial belt of $C_{50}H_{10}$. The optimized structures of all 9 distinct $C_{50}H_8$ isomers are given in Figure 4. DFTB and GGA-DFT computations find the removal of H_2 endothermic, and the isomers where the two H atoms are taken from neighboring sites (1−1 and 1−10) are energetically preferred. As structures with such high strain energies may have open-shell ground states we recomputed the triplet states but find them all energetically less stable than the singlets. These computations demonstrate that the isolated unsaturated carbon atoms at the equatorial belt are penalized by 100 kJ/mol or more.

In summary, we observe a qualitative difference of the stability and electronic structure of the bare and saturated cages

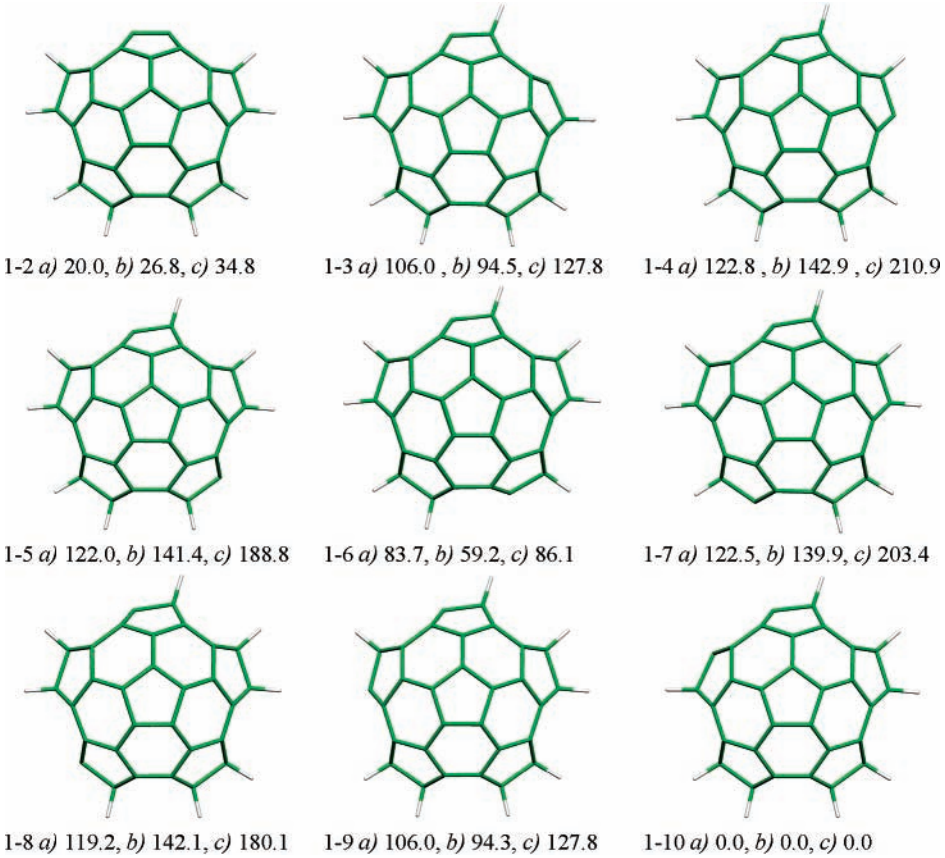

Figure 4. Structures and relative energies of $C_{50}H_8$ isomers. Relative energies are given in kJ/mol at (a) DFTB, (b) PBE/DZVP//DFTB, and (c) B3LYP/6-31G*//DFTB levels.

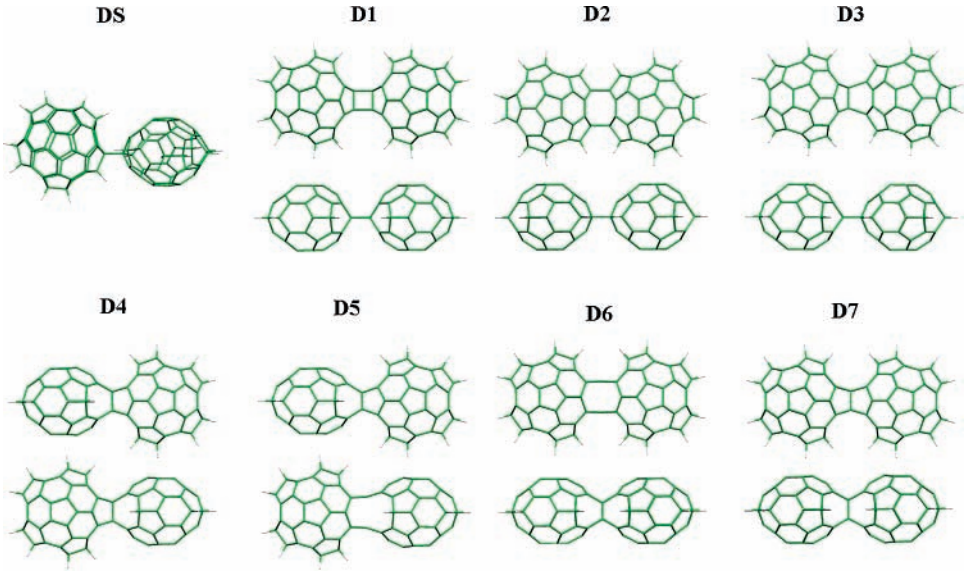

Figure 5. Structures of C_{50} based dimers corresponding to Table 3

TABLE 3: Relative Energies *E* (in kJ mol^{-1}) and Gap Δ (in eV) Energies for the Single-Bonded and the Seven Most Stable Double Bonded Dimers[a]

	DFTB//DFTB				PBE/DZVP//DFTB				B3LYP/6-31G(d)//DFTB			
	E		Δ		*E*		Δ		*E*		Δ	
type of connection	H	B	H	B	H	B	H	B	H	B	H	B
DS		197.6	2.5	0.2		254.3	2.3	0.2		238.5	3.3	0.6
D1	41.6	144.3	2.4	0.8	67.8	164.4	2.2	1.0	85	146.4	3.3	1.7
D2	−4.6	99.2	2.2	1.1	84.8	230.7	1.7	1.0	124	205.1	2.7	1.9
D3	99.8	207.9	2.5	0.9	136.2	251.4	2.2	0.9	171.6	244.7	3.3	1.8
D4	0.0	0.0	2.5	0.5	0.0	0.0	2.4	1.3	0.0	0.0	3.5	1.9
D5	212.5	237.9	1.5	0.5	268.6	270	0.9	0.3	242.6	258.1	2	1.1
D6	13.1	64.3	2.1	0.9	101.7	160.8	1.9	1.0	84.7	151.9	3.0	1.8
D7	26.6	52.4	2.5	1	31.7	160.7	2.3	0.9	69.3	135.3	3.4	1.7

[a] The fully saturated (hydrogenated) structures are indicated by H, the bare cages with B. Energies are given at DFTB//DFTB, PBE/DZVP//DFTB, and B3LYP//6-31G(d)//DFTB levels. The structures are given in Figure 5.

D_{5h} C_{50} and D_{5h} $C_{50}X_{10}$. The saturation of the carbons at the equatorial belt is essential for release of strain energy and stabilization of the π system of the D_{5h} C_{50} cage. Therefore, the formation of dimers and oligomers is investigated both with saturated and bare cages, where bridging bonds are restricted to the chemically active equatorial belt of the molecule. As the unsaturated, partially linked cages are still highly reactive we concentrate mainly on the saturated ones in the discussion.

Dimers. There is one topological possibility for a single-bonded dimer of C_{50}. Single-bonded $(C_{50})_2$, abbreviated with **DS** in Figure 5 and the following, is expected to be instable, as two electrons are taken from the two π systems, resulting in either a biradical or a zwitterion. The reaction

$$2\ C_{50}H_{10} \rightarrow (C_{50}H_9)_2 + H_2$$

is found to be endothermic by 46 kJ/mol. Fully saturated $(C_{50}H_9)_2$, however, maintains its four corannulene-type π systems and has therefore a large HOMO−LUMO gap Δ of 2.3 eV (vs corannulene: Δ = 3.1 eV, for the bare dimer: Δ = 0.2 eV) and is a stable dimer.

There are several possibilities to form dimers of C_{50} bridged by two single bonds. In Table 3, we give the structure of the seven most stable double-bridged dimers of our study. Also, the relative energies and HOMO−LUMO gaps of the bare (unsaturated) dimers and of the hydrogenated (saturated) $(C_{50}H_8)_2$ species are reported in this table. Both, for saturated and unsaturated dimers we find a bridge connecting two e_{55} to a four-membered ring (4MR), with a 90° twisted orientation of the monomers with respect to each other, to be the most stable form **D4** (for structures and nomenclature see Figure 5).

Our computations at various levels of theory and comparison with the results of Lu et al.[19] show that the DFTB geometries correspond to structures with correct relative GGA energies: The PBE/DZVP//DFTB level gives very similar results compared to computationally much more expensive full DFT-GGA geometry optimizations at the B3LYP/6-31G* level. For the dimers studied in ref 19 (**D1**, **D2**, and **D3** in our nomenclature) bond lengths agree within 0.02 Å and relative energies within 8 kJ/mol. Also, the relative energies give the qualitative trend correctly, with one exception: for the saturated dimers, DFTB finds **D2** slightly more stable than **D4**. Therefore, we base our following discussions on the energies of the PBE/DZVP//DFTB computations.

For the unsaturated dimers, **D4** is an extraordinary stable isomer, as the 2nd isomer, **D7**, is 161 kJ/mol higher in energy. In case of the hydrogenated dimers more bridges are competitive in energy: **D1**, **D2**, and **D7** are all in the range of 100 kJ/mol, where the relative energy of **D7** is just 32 kJ/mol higher than **D4**. The closer relative energies of the hydrogenated dimers reflects the important role of the electronic π systems: While it is different for bare monomer and dimer, for the saturated species the dimerization affects only the σ system, and the dimerization energy is mainly determined by the strain differences of monomers and dimer. Isomer **D2** is connected in the

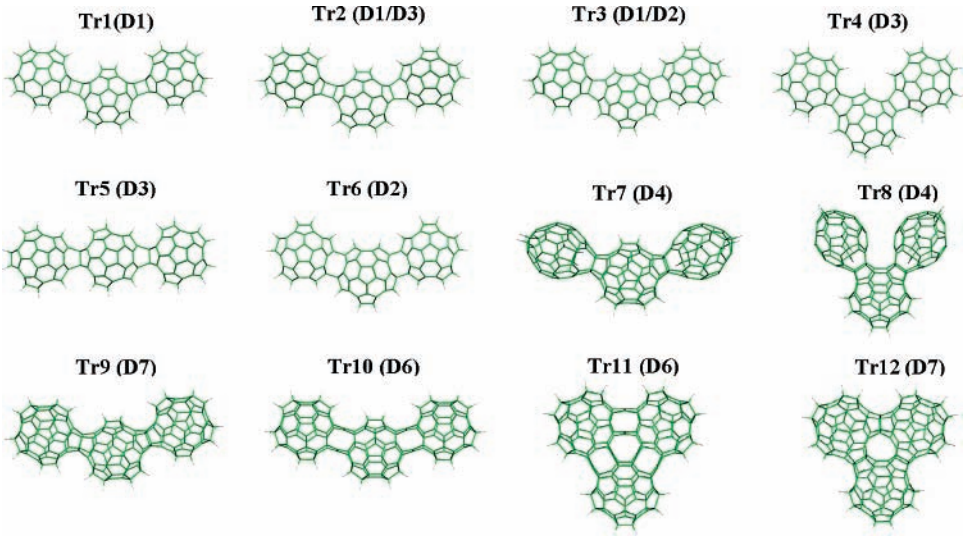

Figure 6. Structures of C_{50} based trimers corresponding to Table 4

same manner as the C_{36} dimer and C_{36} solid discussed earlier.[13,14] In the case of C_{50}, this connection pattern is 85 kJ/mol less stable than **D4**, as it involves a higher strain in the structure. Isomer **D7** is the "untwisted" variant of **D4** and found to be 31 kJ/mol less stable than **D4**.

All reported bare dimers are more stable than the monomers, with energy of formation

$$2C_{50} \rightarrow (C_{50})_2$$

of −486 kJ/mol for unsaturated **D4**. This dimerization energy is about twice as high as for $(C_{36})_2$, and even ∼16 times higher than for the C_{60} dimer. Forming the most stable dimer, **D4**, from $C_{50}H_{10}$ with the reaction

$$2C_{50}H_{10} \rightarrow (C_{50}H_8)_2 + 2H_2$$

gives an endothermic reaction energy of 132 kJ/mol (PBE/DZVP//DFTB).

As for other proposed carbon-based solids as C_{60}, C_{36},[12−14] and C_{20},[16] the connectivity patterns of the dimers are now used for forming hypothetical oligomers of C_{50}-based trimers, tetramers, pentamers, and hexamers. Our computations, in conjunction with experimental evidence,[17] suggest that the building blocks of the oligomers are saturated $C_{50}H_{10}$ units, and we allow single and selected double bridges.

Oligomers and Toward Solid-State Structures. All types of oligomers considered in this article consist of up to six monomer units (C_{50} and $C_{50}H_{10}$), connected with single (**S**) or double bonds (**Dn**, n as introduced in the dimer section). Oligomer structures are constructed by removing the hydrogens from the connecting carbons and placing the structures in such way that interatomic link atoms are formed. This way, clustered and chainlike oligomers are formed (see Figures 6 and 7 for clustered oligomers).

As the number of possible oligomer structures is exceedingly large, we restricted ourselves to the energetically most preferable connectivity patterns of dimer structures, on which successively further monomer structures were added and optimized. Tables 4−7 and Figures 6-7 show the considered oligomer structures, which contain various types of bonding.

As for the dimer, the bare trimer with single bonds has a small HOMO−LUMO gap and hence is of either radicaloid or zwitterionic character. On the other hand, the saturated trimer has a large gap. Structure and electronic structure of each cage unit of the saturated single-bonded trimer do not differ considerably from $C_{50}H_{10}$, and this bonding allows polymerization in an infinite variety of structures, most likely toward amorphous polymers. Therefore, we do not consider more directed oligomers with this bonding pattern and concentrate to those with dimer bridges, which are responsible for most fullerene solids so far observed and discussed.[12,15,35]

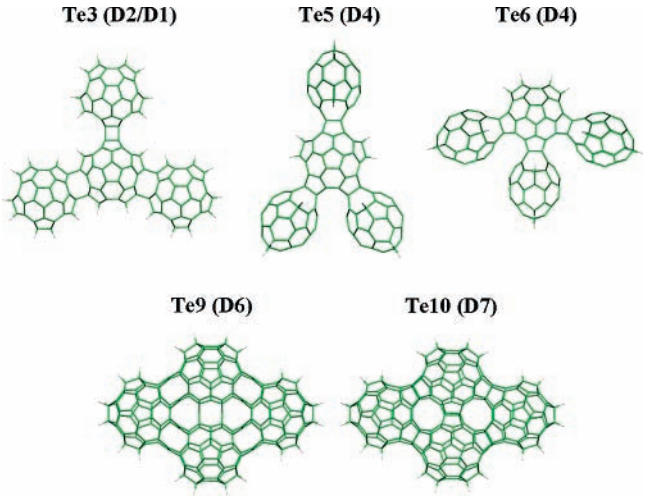

Figure 7. Structures of C_{50} based tetramers corresponding to Table 5

TABLE 4: Relative Energies of C_{50}-Based Trimers (Tr)[a]

		DFTB//DFTB				PBE/DZVP//DFTB			
		E		Δ		*E*		Δ	
structures	type of connection	H	B	H	B	H	B	H	B
TrS	**DS**		364.5	2.5	0.2		416.6	2.0	0.1
Tr1	**D1**	125.5	303.0	2.4	0.8	157.1	320.6	2.1	0.8
Tr2	**D1/D3**	183.6	369.0	2.4	0.8	224.9	411.7	2.1	0.7
Tr3	**D1/D2**	136.9	315.8	2.2	0.9	242.4	436.5	1.6	0.9
Tr4	**D3**	241.1	478.4	2.4	0.5	293.2	551.6	2.1	0.1
Tr5	**D3**	241.5	460.2	2.4	0.5	294.0	497.0	2.1	0.6
Tr6	**D2**	33.1	205.3	2.2	1.2	191.6	413.1	1.6	0.9
Tr7	**D4**	59.0	91.2	2.5	0.8	39.7	62.5	2.4	0.0
Tr8	**D4**	0.0	0.0	2.5	0.5	0.0	0.0	2.3	0.9
Tr9	**D7**	109.1	181.5	2.5	0.6	100.4	126.8	2.2	0.5
Tr10	**D6**	63.9	187.8	2.1	0.5	221.1	350.4	1.9	0.3
Tr11	**D6**		69.0		0.5		338.5		0.9
Tr12	**D7**		−27.2		0.8		−107.7		0.9

[a] Details as in Table 3.

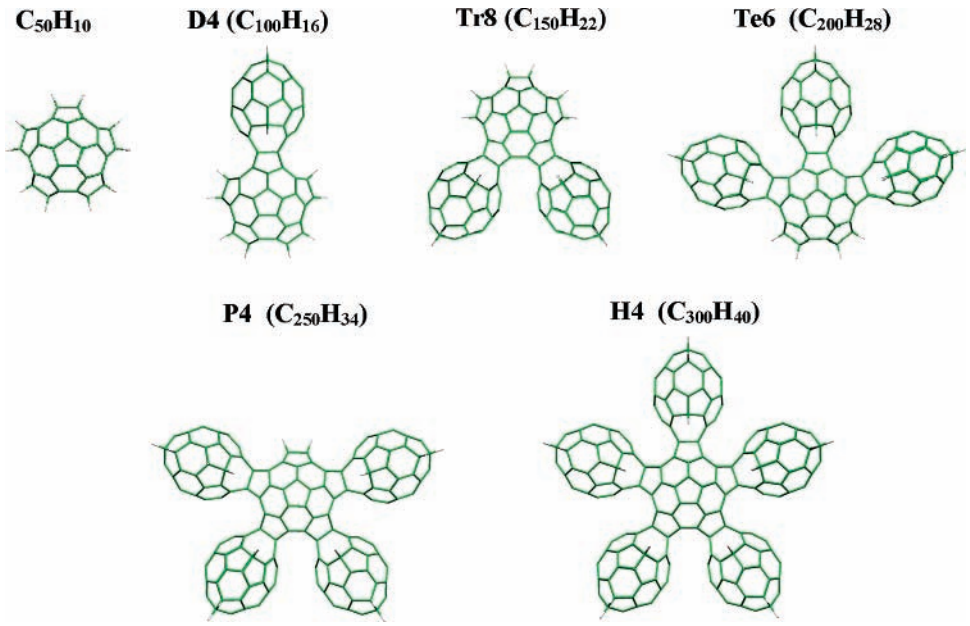

Figure 8. Minimal energy pathway from $C_{50}H_{10}$ to $C_{300}H_{30}$. All of these structures contain only D4 bonding pattern.

TABLE 5: Relative Energies of C_{50}-based Tetramers (Te)[a]

		DFTB//DFTB			
		E		Δ	
structures	type of connection	H	B	H	B
Te1	**D1**	192.4	440.7	2.4	0.7
Te2	**D3**	362.8	688.2	2.4	0.4
Te3	**D2/D1**	95.6	411.2	2.1	0.6
Te4	**D2**	50.3	286.0	2.2	1.2
Te5	**D4**	54.9	45.5	2.5	0.9
Te6	**D4**	0.0	0.0	2.4	0.7
Te7	**D6**	95.1	290.9	2.1	0.3
Te8	**D7**	173.5	284.8	2.5	0.5
Te9	**D6**		527.8		0.3
Te10	**D7**		253.2		0.6

[a] Details as in Table 3.

TABLE 6: Relative Energies of C_{50}-based Pentamers (P)[a]

		DFTB//DFTB			
		E		Δ	
structures	type of connection	H	B	H	B
P1	**D1**	234.5	596.3	2.398	0.673
P2	**D3**	464.5	938.8	2.417	0.393
P3	**D2**	48.5	390.6	2.175	1.181
P4	**D4**	0.0	0.0	2.386	1.036
P5	**D6**	109.5	419.0	2.103	0.254
P6	**D7**	216.0	414.0	2.526	0.499

[a] Details as in Table 3.

Further oligomerization and polymerization gives additional intercage bonds and hence, at least for the bare structures, additional binding energy, but also topological constrains, which lead to unfavorable deformations of the monomer units, which affect both the π system by stronger pyramidalization, and the σ framework. The reaction energy of a further step in polymerization depends mainly in the type of additional intercage bond if this step does not involve strong cage deformations. For this reason, the bonding types found in dimers, oligomers and solids are usually the same, as observed in studies of C_{60},[36−39] C_{70},[40−42] and C_{36}.[13,14] In the case of C_{50} we find exactly the same trend: The energetically favored dimer bridge type **D4** has been found in the two most stable trimers, both for

TABLE 7: Relative Energies of C_{50}-based Trimers (H)[a]

		DFTB//DFTB			
		E		Δ	
structures	type of connection	H	B	H	B
H1	**D1**	316.4	780.3	2.395	0.651
H2	**D2**	84.1	520.9	2.171	1.179
H3	**D3**	603.9	1215.4	2.414	0.369
H4	**D4**	0.0	0.0	2.390	1.032
H5	**D6**	160.4	573.5	2.102	0.222
H6	**D7**	298.3	567.4	2.527	0.492

[a] Details as in Table 3.

saturated and for unsaturated structures. Furthermore, this trend continues to tetramers, pentamers, and hexamers, and a lowest-energy pathway from monomer to hexamer **H4** is found (see Figure 8). Besides being the most stable oligomers, the **D4**-type bonded structures have also large HOMO−LUMO gaps and the tendency to prefer clustered structures. The most stable stretched structures are also based on the **D4** bridge type but energetically less stable.

Oligomers based on the other dimer-like double bonded bridges give also results as expected from the dimer computations. The relatively high stability of the **D2** isomer in the tetramers has to be attributed to the DFTB energy overestimation of this bond type and is probably less stable with higher-level methods. Among the oligomers based on other bridges than **D4** and **D2** especially those of **D3** type of bonding are relatively stable. Relative energies of these isomers are given in Tables 4−7, and selected structures are given in Figures 6 and 7.

Given the 5-fold symmetry of the monomer and the minimum energy pathway to the **H4** hexamer, we conclude that it is impossible to form regular covalently bound C_{50} solids if only the chemically active connectivity sites along the σ_h plane of the molecule are used. The noncovalent interactions between the corannulene units is slightly attractive (6 kJ/mol at the PBE/DZVP//DFTB level). Covalent bonds between a C_2 unit of the equatorial belt and two atoms of a corannulene unit are also possible (the dimerization energy of the most stable bare dimer is 227 kJ/mol, about half the value as for **D4)**. A much larger variety of bonding patterns is hence possible, but thermody-

namically the formation of these bonds is less favored, as it does not saturate the highly reactive sites along the equatorial belt.

Conclusion

The classical C_{50} fullerenes do not agree with the "rule of minimum number of pentagon adjacencies", which is explained by the special structure of C_{50}, which consists of two corannulene units held together with five equatorial C_2 units. The extraordinary stability of $C_{50}Cl_{10}$ and $C_{50}H_{10}$ can be explained by this particular structure: Saturation of the equatorial C_2 units to C_2H_2 units reduces strongly the fullerene strain and allows stable corannulene-type π systems. The cage contains two separated π systems which may cause special magnetic properties similar to C_{60} polymer.[43]

Experimental work on the synthesis of C_{50} polymers is encouraged by our computations but has to face the problem that unsaturated belt carbons are instable and should be saturated, either by a linking bridge, or by a hydrogen or halogen atom. This reduces the possibility of forming spontaneous, high-symmetry solids. Oligomerization and polymerization are energetically possible with single and double bridge links. While single bonded links will lead to flexible intercage bonding, allowing a great manifold of possible structures, double bonded oligomers have a lowest-energy pathway from the monomer over dimer **D4** to a D_{5h} hexamer **H4**.

Acknowledgment. Dr. Z. Chen and Dr. J. Zhao is thanked for fruitful discussion and unpublished information. We thank the Deutsche Forschungsgemeinschaft (DFG) for financial support.

References and Notes

(1) Schmalz, T. G.; Seitz, W. A.; Klein, D. J.; Hite, G. E. *J. Am. Chem. Soc.* **1988**, *110*, 1113.
(2) Kroto, H. **1987**, *329*, 529.
(3) Dresselhaus, M. S.; Dresselhaus, G.; Eklund, P. *Science of Fullerenes and Carbon Nanotubes*; Academic Press: New York, 1996.
(4) *Advanced Series in Fullerenes*; World Scientific Publishing: Singapore, 1995; Vol. 4.
(5) Cioslowski, J. *Electronic structure calculations on fullerenes and their derivatives*; Oxford University Press: Oxford, U.K., 1995.
(6) Heine, T. Fullerenes. In *Calculation of NMR and EPR Parameters: Theory and Applications*; Kaupp, M., Bühl, M., Malkin, V. G., Eds.; Wiley-VCH: Weinheim, Germany, 2004.
(7) Kietzmann, H.; Rochow, R.; Ganteför, G.; Eberhardt, W.; Vietze, K.; Seifert, G.; Fowler, P. W. *Phys. Rev. Lett.* **1998**, *81*, 5378.
(8) Piskoti, C.; Yarger, J.; Zettl, A. *Nature* **1998**, *393*, 771.
(9) Prinzbach, H.; Weller, A.; Landenberger, P.; Wahl, F.; Worth, J.; Scott, L. T.; Gelmont, M.; Olevano, D.; von Issendorff, B. *Nature* **2000**, *407*, 60.
(10) Koshio, A.; Inakuma, M.; Sugai, T.; Shinohara, H. *J. Am. Chem. Soc.* **2000**, *122*, 398.
(11) Koshio, A.; Inakuma, M.; Wang, Z. W.; Sugai, T.; Shinohara, H. *J. Phys. Chem. B* **2000**, *104*, 7908.
(12) Menon, M.; Richter, E. *Phys. Rev. B* **1999**, *60*, 13322.
(13) Fowler, P. W.; Heine, T.; Rogers, K. M.; Sandall, J. P. B.; Seifert, G.; Zerbetto, F. *Chem. Phys. Lett.* **1999**, *300*, 369.
(14) Heine, T.; Fowler, P. W.; Seifert, G. *Solid State Commun.* **1999**, *111*, 19.
(15) Menon, M.; Richter, E.; Chernozatonskii, L. *Phys. Rev. B* **2000**, *62*, 15420.
(16) Chen, Z. F.; Heine, T.; Jiao, H. J.; Hirsch, A.; Thiel, W.; Schleyer, P. V. R. *Chem.-A Eur. J.* **2004**, *10*, 963.
(17) Xie, S. Y.; Gao, F.; Lu, X.; Huang, R. B.; Wang, C. R.; Zhang, X.; Liu, M. L.; Deng, S. L.; Zheng, L. S. *Science* **2004**, *304*, 699.
(18) Chen, Z. F. *Angew. Chem. Int. Ed.* **2004**, *43*, 4690−4691.
(19) Lu, X.; Chen, Z. F.; Thiel, W.; Schleyer, P. v. R.; Huang, R. B.; Zheng, L. *J. Am. Chem. Soc.* **2004**, *126*, 14871.
(20) Wang, Z. X.; Ke, X. Z.; Zhu, Z. Y.; Zhu, F. Y.; Ruan, M. L.; Chen, H.; Huang, R. B.; Zheng, L. S. *Phys. Lett. A* **2001**, *280*, 351.
(21) Hitoshi, G. *Fullerene Structure Library*, 1998.
(22) Fowler, P. W.; Manolopoulos, D. E. *An Atlas of Fullerenes*; Clarendon Press: Oxford, U.K., 1996.
(23) Porezag, D.; Frauenheim, T.; Kohler, T.; Seifert, G.; Kaschner, R. *Phys. Rev. B* **1995**, *51*, 12947.
(24) Perdew, J. P.; Burke, K.; Ernzerhof, M. *Phys. Rev. Lett.* **1996**, *77*, 3865.
(25) Godbout, N.; Salahub, D. R.; Andzelm, J.; Wimmer, E. *Can. J. Chem.-Rev. Can. Chim.* **1992**, *70*, 560.
(26) Köster, A. M.; Goursot, G. G.; Heine, A.; Salahub, T.; Vela, D. R.; Patchkovskii, A. V. *deMon 2003*; NRC: Ottawa, 2003.
(27) Frisch, M. J.; Trucks, G. W.; Schlegel, H. B.; Scuseria, G. E.; Robb, M. A.; Cheeseman, J. R.; Zakrzewski, V. G.; Montgomery, J. A., Jr.; Stratmann, R. E.; Burant, J. C.; Dapprich, S.; Millam, J. M.; Daniels, A. D.; Kudin, K. N.; Strain, M. C.; Farkas, O.; Tomasi, J.; Barone, V.; Cossi, M.; Cammi, R.; Mennucci, B.; Pomelli, C.; Adamo, C.; Clifford, S.; Ochterski, J.; Petersson, G. A.; Ayala, P. Y.; Cui, Q.; Morokuma, K.; Malick, D. K.; Rabuck, A. D.; Raghavachari, K.; Foresman, J. B.; Cioslowski, J.; Ortiz, J. V.; Stefanov, B. B.; Liu, G.; Liashenko, A.; Piskorz, P.; Komaromi, I.; Gomperts, R.; Martin, R. L.; Fox, D. J.; Keith, T.; Al-Laham, M. A.; Peng, C. Y.; Nanayakkara, A.; Gonzalez, C.; Challacombe, M.; Gill, P. M. W.; Johnson, B. G.; Chen, W.; Wong, M. W.; Andres, J. L.; Head-Gordon, M.; Replogle, E. S.; Pople, J. A. *Gaussian 98*, revision A.7; Gaussian, Inc.: Pittsburgh, PA, 1998.
(28) Wen Guo Xu, Y. W., Qian Shu LI. *J. Mol. Struct. (THEOCHEM)* **2000**, *531*, 119.
(29) Jones, R. O. *J. Chem. Phys.* **1999**, *110*, 5189.
(30) Albertazzi, E.; Domene, C.; Fowler, P. W.; Heine, T.; Seifert, G.; Van Alsenoy, C.; Zerbetto, F. *Phys. Chem. Chem. Phys.* **1999**, *1*, 2913.
(31) Slanina, Z.; Zhao, X.; Osawa, E. *Chem. Phys. Lett.* **1998**, *290*, 311.
(32) Slanina, Z.; Uhlik, F.; Zhao, X.; Ueno, H.; Osawa, E. *Fullerene Sci. Technol.* **2000**, *8*, 433.
(33) Slanina, Z.; Uhlik, F.; Zhao, X.; Osawa, E. *J. Chem. Phys.* **2000**, *113*, 4933.
(34) Heine, T.; Fowler, P. W.; Rogers, K. M.; Seifert, G. *J. Chem. Soc.-Perkin Trans. 2* **1999**, 707.
(35) Collins, P. G.; Grossman, J. C.; Cote, M.; Ishigami, M.; Piskoti, C.; Louie, S. G.; Cohen, M. L.; Zettl, A. *Phys. Rev. Lett.* **1999**, *82*, 165.
(36) Nagel, P.; Pasler, V.; Lebedkin, S.; Soldatov, A.; Meingast, C.; Sundqvist, B.; Persson, P. A.; Tanaka, T.; Komatsu, K.; Buga, S.; Inaba, A. *Phys. Rev. B* **1999**, *60*, 16920.
(37) Scuseria, G. E. *Chem. Phys. Lett.* **1996**, *257*, 583.
(38) Scuseria, G. E.; Xu, C. H. *Phys. Rev. Lett.* **1995**, *74*, 274.
(39) Porezag, D.; Jungnickel, G.; Frauenheim, T.; Seifert, G.; Ayuela, A.; Pederson, M. R. *Appl. Phys. A-Mater. Sci. Proc.* **1997**, *64*, 321.
(40) Soldatov, A. V.; Roth, G.; Dzyabchenko, A.; Johnels, D.; Lebedkin, S.; Meingast, C.; Sundqvist, B.; Haluska, M.; Kuzmany, H. *Science* **2001**, *293*, 680.
(41) Lebedkin, S.; Hull, W. E.; Soldatov, A.; Renker, B.; Kappes, M. M. *J. Phys. Chem. B* **2000**, *104*, 4101.
(42) Heine, T.; Zerbetto, F.; Seifert, G.; Fowler, P. W. *J. Phys. Chem. A* **2001**, *105*, 1140.
(43) Makarova, T. L.; Sundqvist, B.; Hohne, R.; Esquinazi, P.; Kopelevich, Y.; Scharff, P.; Davydov, V. A.; Kashevarova, L. S.; Rakhmanina, A. V. *Nature* **2001**, *413*, 716.